

THE DEVELOPMENT OF GAS/STAR OFFSETS IN TIDAL TAILS

J. CHRISTOPHER MIHOS¹

To appear in the Astrophysical Journal

ABSTRACT

We present models of interacting galaxies in order to study the development of spatial offsets between the gaseous and stellar components in tidal tails. Observationally, such offsets are observed to exist over large scales (e.g., NGC 3690; Hibbard et al. 2000), suggesting an interaction between the tidal gas and some (unseen) hot ISM. Instead, our models show these offsets are a natural consequence of the radially extended H I spatial distribution in disk galaxies, coupled with internal dissipation in the gaseous component driven by the interaction. This mechanism is most effective in systems involved in very prograde interactions, and explains the observed gas/star offsets in interacting galaxies without invoking interactions with a hot ISM, starburst ionization, or dust obscuration within the tails.

Subject headings: galaxies: interactions, galaxies: ISM, galaxies: kinematics and dynamics

1. INTRODUCTION

Since the original work of Toomre & Toomre (1972) and Wright (1972), it has been recognized that the development of tidal tails during galaxy encounters is predominantly a kinematic effect – stars are tidally torn away from the parent galaxy and orbit as “test particles” in the evolving potential. While self-gravity and hydrodynamic forces can play a significant role in the development of substructure *within* tidal debris (see, e.g., Wallin 1990; Barnes & Hernquist 1992; Elmegreen, Kaufman, & Thomasson 1993), the *global* evolution of tidal tails is much simpler. Because both gas and stars respond to the gravitational potential in a similar fashion, they should have similar kinematics and spatial morphology on large scales. To be sure, differences exist between the mass distribution of stars and gas in tidal tails – gaseous tails are often much more extended than their stellar counterparts – but this is due largely to the differing radial distribution of stars and gas in the parent galaxy. Because H I disks extend further out than stellar disks (e.g., Broeils & van Woerden 1994; Broeils & Rhee 1997), there is more loosely bound gas to be ejected to large distances in the tidal debris. Nonetheless, the kinematic nature of the process predicts that when material is tidally ejected, stars and gas should remain largely cospatial in the resulting tidal tails.

Observationally, this situation holds true in many cases. Examples of cospatial gas/star tails include nearly all the nearby mergers such as the Antennae, NGC 7252, or NGC 4676 (Hibbard & van Gorkom 1996). This coevolutionary status of tidal gas and stars permits detailed matching between the theoretic predictions of stellar-dynamical models and the observed morphology and kinematics of the gas. Several investigators have taken advantage of this fact to produce dynamical models of specific merging systems (e.g., Stanford & Balcells 1991; Mihos et al. 1993; Hibbard & Mihos 1995; Yun 1999; Barnes & Hibbard 2000).

However, in a significant number of systems the H I and stellar tidal debris are not purely cospatial. In many of these cases, the observed gas/star offsets can be explained, at least qualitatively, by interpenetrating events

during galaxy collisions. For example, the offset in the tidal bridge of NGC 7714/5 (Smith et al. 1997) is reasonably expected to occur since tidal bridges form from material on the interface between two interacting galaxies; collisional shocks will act to strip gas material out of the developing tidal bridge. In retrograde encounters, short tails and plumes form from material which passes entirely through the companion galaxy, leading to a strong decoupling of the stars and gas (compare, for example, Figures 11 and 12 of Mihos & Hernquist 1996). In yet other cases, offsets can be attributed to the fact that tidal material has fallen back through the merging galaxies and may be subject to additional dissipation, as perhaps seen in the offset stellar and gaseous “shells” in Centaurus A (Schiminovich et al. 1994).

However, these explanations cannot account for a small number of cases in which offsets exist between the gas and stars in extended tidal tails. Notable examples include the tidal tails of NGC 520 (Hibbard, Vacca, & Yun 2000), 7714/5 (Smith et al. 1997), and, most dramatically, NGC 3690 (Hibbard & Yun 1999), in which the gas and stars show an offset of ~ 20 kpc over much of the ~ 180 kpc extent of the tail. In these examples, none of the previously mentioned mechanisms easily explains the observed offsets. These are all examples of long tidal tails, which develop from the side of the galaxy *away* from the companion and do not therefore come in physical contact with the companion. Unlike the tidal shells and loops in older mergers, the long tails here have not yet fallen back through their central objects, and, furthermore, the length of the tails precludes a retrograde geometry for the encounter.

At face value, these observations call into question the idea that the evolution of tidal tails is purely kinematic, and suggest that hydrodynamic forces may also play a role in the global evolution of the tidal tails. Hibbard et al. (2000) suggest that the offsets may arise from a variety of effects, including ionization of part of the tail from a starburst wind or from the stars in the tail itself, partial obscuration by dust in the tail, or by an interaction between the tidal gas and a hot ISM component, either a hot gaseous halo or a starburst wind. However, many of these

¹Department of Astronomy, Case Western Reserve University, 10900 Euclid Ave, Cleveland, OH 44106, hos@burro.astr.cwru.edu

solutions seem somewhat contrived, particularly with respect to the case of NGC 3690. In this case, the gas appears to lead the stellar tail, whereas a gas tail expanding into a hot halo would tend to trail its stellar counterpart. A starburst wind solution is also difficult to envision, as the wind would need to be extremely collimated over very large scales to result in such an extended, linear offset. While ROSAT observations of NGC 3690 (Heckman et al. 1999) do show evidence for a hot outflow, but the X-ray isophotes exist on scales much smaller than needed to explain the offset tidal gas (~ 45 kpc compared to the 180 kpc extent of the tidal tail). While the starburst wind may extend to even larger radii at lower temperatures and densities, there is no direct evidence for such an extended outflow.

In this paper we describe a simpler solution for the observed gas/star offsets in some tidal tails. In this model, the offsets arise from the differing radial distributions of gas and stars, coupled with interaction-driven dissipation and inflow in the tidal gas. This scenario explains the observed offsets without resorting to esoteric processes such as hot ISM interactions, starburst ionization, or dust obscuration.

2. INTERACTION MODEL

To explore the physics which might lead to gas/star segregation in tidal debris, we use numerical modeling of galaxy mergers to follow the kinematic evolution of both the stellar and gaseous components of tidal features. The models are calculated using an N-body treecode coupled with smoothed particle hydrodynamics to follow the evolution of the gas (TREESPH; Hernquist & Katz 1989). The galaxy models consist of a composite disk/bulge/halo system, in which the disk is exponential with mass $M_d = 1$ and radial scale length $h = 1$, the bulge is a flattened Hernquist model with mass $M_b = 1/3$, scale radius $a = 0.4$ and axial ratio $b/a = 0.5$, and the halo is a truncated isothermal sphere of mass $M_h = 5.8$, core radius $r_c = 1.0$, and tidal radius $r_t = 10.0$ (see Hernquist 1993 and MH96 for more details). In these units, one half mass rotation period for the disk is 12 units of time, and scaling the model to the Milky Way gives length, mass, and time scale factors of 3.5 kpc, $5.6 \times 10^{10} M_\odot$, and 13 Myr respectively.

The model we present here is identical to the fiducial model of Mihos & Hernquist (1994, 1996), with one significant difference. In those previous models, the gas was distributed exponentially in the disk, with a radial scale length equal to that of the stellar disk and a total mass of $M_g = 0.1M_d$. Those models were designed to study inflow and nuclear starbursts, and the gas distribution was chosen to mimic the molecular gas distribution in spiral galaxies. However, the H I in galaxies is typically much more extended than the starlight, so that the gas distribution used in those models was a poor representation of the gas likely to be ejected in tidal debris. To rectify this shortcoming, the models presented here use a different gas mass distribution: the gas is exponential out to a radius of $2.5h$, after which it follows a r^{-1} surface density distribution out to a truncation radius of $8h$. Because of the more slowly declining gas distribution at large radius, Model B has a higher gas mass: $M_g = 0.25M_d$. Conceptually, Model B represents a more realistic gas distribution; the inner exponential distribution mimics the molecular gas content in

galaxies, while the extended HI gas is represented by the slower drop off in density at large radius. The relatively high gas fraction in this model $M_g = 0.25M_d = 0.05M_{dyn}$ is more typical of late type Sb or Sc galaxies than luminous Sa's (see compilations by Young & Scoville 1991; Roberts & Haynes 1994; McGaugh & de Blok 1997). However, given the large gas content and high M_g/L_B ratios of systems like NGC 3690 which show gas/star offsets in their tidal debris, late-type spirals are in fact the likely progenitors of such systems (e.g., Hibbard et al. 2000).

The merger we simulate is again identical to the fiducial merger of MH96 – a merger between two equal mass disk galaxies, placed on an initially parabolic orbit with pericentric distance of $r_{peri} = 2.5h$. One disk is exactly prograde ($i = 0^\circ$), while the second is highly inclined to the orbital plane ($i = 71^\circ, \omega = 30^\circ$). Figure 1 shows the evolution of the gas and stars in the simulation. As the galaxies first pass one another, the tidal tails are launched and the galaxies move apart, reaching a maximum separation of $\sim 15h$ before turning around on their orbit and merging together. In terms of the global dynamics (morphology, kinematics, and timescales) this model evolves nearly identically to that of MH96; more details on the global evolution and the triggering of nuclear gas flows can be found in Mihos & Hernquist (1994) and MH96.

However, while the global evolution of this model is similar to that of MH96, on smaller scales striking differences exist between the tidal features of the two models. In MH96, the gas and stars in the two tails are cospatial, while here they exhibit strong differences. In the prograde tail the gas is significantly offset from the stars – and in fact leads the stellar tail – while the inclined tail shows a clear bifurcation in the gaseous component. Neither of these features are seen in the MH96 tails (see Figures 3 and 4 of MH96). The gas-leading prograde tail in the current model captures many of the features of the tail in Arp 299, including both the gas/star offset and the fact that the gas and stars become cospatial again at the end of the tail.

Figure 1 alone is enough to weaken models for gas/star offsets which propose interactions between tail gas and a hot ISM or ICM; since no such hot gaseous phase is present in these models, it is not a necessary condition for gas/star segregation. Similarly, starburst outflows are not necessary, nor is *in-situ* ionization of the gas from the stellar component of the tails. In fact, given the restricted set of physics modeled in the simulation, the offsets must be explainable either by the simple differences in spatial distribution of gas and stars in the progenitor disks, or by the hydrodynamic effects which occur within the gaseous disks. We now examine the development of the tidal tails in detail to separate these two effects.

3. KINEMATICS OF EXTENDED MASS DISTRIBUTIONS

To decouple hydrodynamic effects from those due to an extended disk of material, a second model was run, identical to the first except that all the gas particles were converted into collisionless stellar particles. The evolution of these collisionless “pseudo-gas” particles is not meant to mimic the evolution of gas, but simply to ask whether an extended mass distribution could result in spatial offsets from a purely kinematic evolution. We leave the question of whether or not it could evolve that way when hydrody-

dynamic effects are included to the following section, which studies the full hydrodynamic evolution of the extended gas disks. For the current exercise, Figure 2 compares the distribution of stars and collisionless pseudo-gas in the galaxies late in the interaction where the offset had developed in the full hydrodynamic model (cf. the final frame of Figure 1).

Although differences can be seen in the distribution of stars and pseudo-gas, the two populations clearly coexist throughout the tails. Pseudo-gas both leads and trails the stellar tail, forming a sheath around the stellar tails. This distribution is similar to that seen in other models of interacting systems, and in fact can be seen in the original collision models of Toomre & Toomre (1972), where rings of particles from subsequently larger initial radii formed tails which were both longer and broader. This result was further explored in Mihos et al. (1998), who examined the evolution of extended test particle distributions in tidal debris, and showed in more detail how material from large radius forms broader, more extended tidal sheath. The difference between those models and the collisionless model shown in Figure 2 is that in the latter model the pseudo-gas is distributed at all radii, so that the sheath around the stellar tails is filled in by pseudo-gas from the inner regions of the disk. The bottom panels of Figure 2 show this more clearly, comparing the distributions of the inner and outer pseudo-gas, where “inner” and “outer” are defined by gas initially interior or exterior to the radius at which the initial gas distribution changed from an exponential to a r^{-1} distribution. Again, the outer pseudo-gas does not lead the stellar tails, but rather is distributed throughout.

While the inclusion of an extended component in the galaxy results in material which leads the stellar tails, it also produces a trailing component – again, the extended pseudo-gas is found in a broader sheath surrounding the stellar component. Comparing such a configuration to observed H I tails is a bit difficult, as there are no hydrodynamical effects included in this collisionless calculation. Certainly one expects that on small scales H I should be more concentrated along the tails, as dissipation acts to keep the internal velocity dispersion of the gas low. On the other hand, on larger scales this calculation argues that a more extended gas distribution could in principle lead to a more diffuse, extended distribution of tidal gas than is suggested by the stellar tidal tails (see, for example, H I imaging of the Antennae by Hibbard & von Gorkom 1996). Any deeper inference must appeal to models which include hydrodynamic effects, which we address in the next section. However, what is clear is that, by itself, an extended spatial distribution of gas does not result in the strong gas/star offset observed in the full hydrodynamic model, or in the tidal tail of Arp 299. Hydrodynamical effects internal to the galaxies must play a role in the formation of these offsets.

4. HYDRODYNAMICAL EFFECTS

The collisionless model demonstrates that extended mass distributions alone cannot be the entire explanation for offset tidal debris. We now examine the role that hydrodynamical effects play in the evolution of the tidal debris. Naively, one might expect a simple comparison of the models with and without gasdynamics (i.e. the models of Figures 1 and 2) would reveal how gas physics have shaped

the evolution of the tail particles. In practice, however, it is not that simple – due to dissipation in the extended and relatively massive gas disks drives further orbital decay, making the hydrodynamic model merge slightly faster than the collisionless one. As a result, the tails in each model evolve slightly differently, making a direct comparison difficult.

To alleviate this problem and study the evolution of the tails in more detail, we introduce the concept of “phase space partners.” We focus on the prograde tail, and isolate gas and star particles within a small piece of the tail where the gas/star offset is most dramatic (Figure 3a). We then examine the model at a time one half rotation period *before* the initial collision and locate the identified particles in their preencounter position (Figures 3b,c). For each particle, we find the particle from the other component nearest to it in phase space, i.e. for each gas particle i we find the star particle j with the minimum phase space distance Δ_{ij} where

$$\Delta_{ij}^2 = \frac{|\vec{x}_i - \vec{x}_j|^2}{h^2} + \frac{|\vec{v}_i - \vec{v}_j|^2}{v_c^2}$$

where h is the disk scale length and v_c is the circular velocity. Because of the large particle number in the model (a total of 65,536 disk particles and 24,576 gas particles in each disk), the phase space separation between the chosen particles and their partners is very small. This ensures that comparing the evolution of the gas particles and their stellar partners are tracking nearly identical phase space origins. By comparing the evolution of the particles and their partners we can thus separate the stellar dynamical evolution of the gas particles from their hydrodynamical evolution.

We begin by showing the evolution of the selected gas and star particles which eventually form the scrutinized portion of the tail (Figure 3d). Before the encounter they are wound into the disk; as the galaxies approach one another the isolated particles unwind until the moment of perigalacticon. At this point, gas and stars are both spatially and kinematically coincident; however, shortly thereafter the gas particles overtake and lead the stellar particles, forming the offset tails. The thickness of the tails reflects their random velocities; the compression of the gas at perigalacticon effectively dissipates the random kinetic energy injected by the collision, so that the gas tail is thinner than the stellar tail.

We next compare the evolution of the gas particles with their stellar phase space partners (Figure 3e). Again, this comparison shows how the gaseous component would have evolved in the absence of hydrodynamic forces. Two things are apparent from this exercise. First, the distribution of gas particles is more compact than that of their stellar partners; again, dissipation has acted to damp out random motion and cause the gas to evolve more cohesively. Second, the gas particles and their stellar partners are essentially cospatial – no offset exists between the components. Hydrodynamic forces act to compress the gas but do not accelerate it; there is no net force applied to the gas (e.g., from other gas particles in the simulation). The gas in this portion of the tidal tail is moving on an essentially collisionless trajectory.

If the tidal gas is acting collisionlessly on large scales,

then why is it offset from the collisionless stellar particles? In other words, why is the stellar tail gas poor – what happened to the gas that should have tracked with the stellar tidal tails? Figure 3f shows the evolution of the stars and their gaseous phase space partners. Shortly after collision, the gas partners begin to fall back in towards the inner regions of their host galaxy, unlike the stars which continue to expand outwards. Because of the exponential distribution of stars, the partner gas comes from the inner regions of the disk, where it is more subject to the dissipation which drives radial inflows (e.g., MH96, Barnes & Hernquist 1996). The gas which would have been co-spatial with the stellar tidal tails has lost energy and angular momentum and has decoupled from the stellar tidal debris.

Figure 4 directly compares the energy and spin angular momentum content (with respect to the center of the parent galaxy) for the different subsamples of tail particles. Comparing the gaseous and stellar components, we see that, as expected due to its initially larger radii, the gas starts out less tightly bound and with higher angular momentum than the stars. After the galaxies initially collide ($T \sim 30$), the tidal tails are ejected and both gas and stars end up with a net increase in angular momentum and decrease in binding energy. The path each component takes is markedly different, however. The stars become transiently more bound as they fall into the potential well of the companion, after which they gain energy through the spin-orbit coupling of the interaction and form the tidal tail. In contrast, the gas gains energy monotonically and moves smoothly into the tidal tail. (Recall here that the gas and star subsets sample different regions of initial phase space, so their evolutionary history can be quite different even though they end up near each other in the resulting tails.)

Comparing the energy and angular momentum for the gas and its stellar partners, the values track very tightly together, reflecting the largely collisionless global evolution of the tidal gas. However, we again see significant differences between the stars and their gas partners, in that as the tails begin to form, the gas partners decouple from the stellar component, losing energy and angular momentum and flowing inwards. Note that the decoupling occurs not at the moment of closest approach – which might be expected if the decoupling was due to shocks from the interpenetrating ISMs – but after the collision, when the galaxy develops a strong self-gravitating response to the collisional perturbation. This result is consistent with the idea that gas loses angular momentum as a result of the internal response of the disk, driven inwards by gravitational torques from the stellar bar and spiral features (see, e.g., Barnes & Hernquist 1991, 1996; Mihos & Hernquist 1996). Once the galaxies finally merge (at $T \sim 65$) further decoupling occurs as gas is again driven inwards due to the merging process.

In summary, then, the gas/star offset observed in the models arises due to a combination of the different spatial distribution of gas and stars in the disk and the collisional evolution of the gaseous component. However, it is not the hydrodynamics of the gas present in the tails which drives the decoupling; rather, it is the evolution of the gas which *would* have been in the tails, but was driven inwards by the collision which shapes the offset. In this sense, the formation of the offset is again an internal response of the

galaxies involved, rather than due to subsequent evolution of the tidal debris. Certainly the offset is not due to any hydrodynamic interaction between the tail gas and any other gaseous component such as a hot halo or IGM.

5. GEOMETRICAL EFFECTS

The previous discussion has focussed on the prograde tail, coming from the disk whose rotational plane matched the orbital plane of the encounter. Since for this galaxy the encounter is exactly prograde ($i = 0^\circ$), the response of the disk is maximized, both in the ejection of tidal tails and the onset of dissipational inflows. Studies of developing caustics in tidal tails show their strong dependence on disk inclination (Wallin 1990). In encounters where the perturbation acts entirely in the disk plane, as in a purely prograde encounter, the developing caustics lead to strong shocks and density enhancements in the gas. If the encounter is more inclined, the caustics become more three dimensional, reducing the effects of the caustic-driven shocks. It is natural therefore to ask how sensitive our result is to varied encounter geometries, and we assess this by examining the structure of the tail in the more inclined ($i = 71^\circ$) disk.

Figures 5a-c shows the inclined tail projected onto the disk plane of its host galaxy. Unlike the morphology of the prograde tail, the inclined tail shows gas distributed across the tidal tail, with a spatial spread similar to that of the stellar component (as seen, for example, in Figure 2). Further inspection, however, reveals an interesting twist to tidal tail formation – the inclined tail actually shows a somewhat bifurcated structure. This bifurcation is due in part to material from the prograde companion which has been accreted by the inclined host galaxy and has formed a secondary, slightly trailing tidal tail. Material in this secondary tail is a mixture of original and accreted material, while the leading tail consists solely of material from the original disk. This mixing of tidal debris from the two galaxies into a single tail could in principle lead to peculiar abundance patterns in tidal tails, which could host material with a range of abundances from different progenitors.

Although a significant fraction of gas in the interior portion of the inclined tail has been accreted from the prograde companion, the majority of the gas in the tail comes from the host galaxy. In other words, the lack of an observed gas/star offset is not because the gas tail has been filled in via accretion, but rather because the offset never developed in the inclined tail. An edge-on view of the inclined tail (Figure 5d-e) shows how the tail has warped out of its original disk plane, reducing the effects of collisional shocks at driving inflow along the tail. The lower angular momentum gas which was easily driven inwards in the prograde tail now remains largely in place in the inclined tail. Geometry does thus play a role in the establishment of offsets by altering the efficiency at which the inner gas decouples from the developing tidal tail. This argues that tails which show a marked offset – such as that in Arp 299 – probably arise from encounters in which the host disk was very prograde.

6. DISCUSSION

The fact that we can account for the offset between the gas and stars in tidal tails without the need for a separate

hot ISM component argues against these offsets necessarily arising from interactions with gaseous halos or starburst winds. We emphasize here that the initial conditions are far from being contrived; on the contrary, the radial distribution of H I in galaxies is typically much more extended than the stellar component (e.g., Broeils & van Woerden 1994; Broeils & Rhee 1997). In truth, the extended gas disk in our model is a more realistic initial galaxy model than those used by MH96 or Barnes & Hernquist 96, where purely exponential gas distributions were used. In essence, better initial conditions have yielded a more accurate description of the formation and evolution of the tidal tails, showing the natural development of the gas/star offset.

These models indicate that the offset is produced when the tail comes from a very prograde encounter; if the encounter is fairly inclined, the dissipation in the gas component is reduced and the offset inhibited. How does this prediction relate to the observed H I properties of mergers? Most nearby mergers do not show strong offsets, consistent with the idea that the geometry must be fairly specific to yield offsets. In two of the more extreme examples of tidal offsets – NGC 3690 and NGC 520 – the orbital geometry inferred from the measured kinematics of the system suggests a prograde encounter (Hibbard et al. 2000), although with significant uncertainties in the exact geometry. If our explanation of the offset holds true, our constraints on the geometry are even more severe than those inferred from the global kinematics of these systems.

Our model also explains the fact that the offset gas tail in NGC 3690 appears to curve back onto the optical tail at large radius (the “hook” described by Hibbard & Yun 1999). Material in the tail at large radius comes from the most loosely bound material at initially large radius in the progenitor disk. Coming from the outskirts of the disk, this material is less susceptible to the inflow driven by the self-gravitating response of the host stellar disk. This material develops in an almost purely collisionless evolution so that the stars and gas remain cospatial. It is only further inwards along the tail that the offset develops, since it is here where the tidal material would have come from deeper in the progenitor galaxy, and be more prone to dissipative effects.

Given the different spatial distributions of gas and stars in the tidal tails, it is also interesting to ask if we see kinematic segregation between the components as well. This has particularly important ramifications for the frequent exercise of modeling specific galaxies based on H I or H α velocity fields. Because of the increased computational

cost of running hydrodynamic simulations, collisionless N-body models are typically used to match the observed (gas-phase) velocities (e.g., Stanford & Balcells 1991; Mihos et al. 1993; Hibbard & Mihos 1995; Yun 1999; Barnes & Hibbard 2000). If severe kinematic segregation exists in the tidal debris, models derived from matching collisionless kinematics to gas velocities may be in serious error. To examine this possibility, Figure 6 shows a simulated position-velocity plot for both the gas and stars, observed in the plane of the prograde tail such that the portion of prograde tail which shows the offset moves directly towards the observer. This viewing geometry results in the *maximum* observed kinematic offset between the stars and gas in the prograde tail. These position-velocity plots show that the kinematic offsets are observable, with offset amplitudes of $\sim 50\text{--}70\text{ km s}^{-1}$, but that they do not radically affect the inferred global kinematics of the system. While detailed model-data matching may hint at differences between the stellar and gas kinematics (see, for example, the discussion in Hibbard & Mihos 1995), the derived models should not be seriously misled by these effects.

Finally, we emphasize that our explanation of gas/star offsets in tidal debris is not the only possible mechanism which may produce offsets. Certainly many examples exist of kinematic decoupling which occurs when the encounter draws tidal material through the inner portions of galaxies, such as retrograde encounters or late infall from tidal tails. The anti-correlation noted by Hibbard et al. (2000) between gas and stars in the tidal debris around Arp 220 are one possible example of this situation, where the stubby tidal features seen in the optical are most likely not due to an extremely prograde encounter. Also, as Hibbard et al. (2000) point out in their discussion of gas/star offsets, many interacting galaxies possess strong starburst winds (Heckman, Armus, & Miley 1987, 1990) and models suggest that collisionally heated halo gas may exist (Barnes & Hernquist 1996); the interaction between the tidal H I and these hot gas components may yet be significant in some cases. What our model shows is that the observed offsets in long tidal tails are easily explained without the need for a hot component, but they do not rule out the presence – or even the effects – of such a hot component.

I thank Lars Hernquist and John Hibbard for many useful discussions. This work is supported through a grant of computing time from the San Diego Supercomputer Center, and by the National Science Foundation through a CAREER Fellowship grant #9876143.

REFERENCES

- Barnes, J.E., & Hernquist, L. E. 1991, ApJ, 370, L65
 Barnes, J.E., & Hernquist, L. 1992, Nature, 360, 715
 Barnes, J.E., & Hibbard, J.E. 2000, in preparation
 Broeils, A. H. & van Woerden, H. 1994, A&AS, 107, 129
 Broeils, A. H. & Rhee, M.-H. 1997, A&A, 324, 877
 Elmegreen, B. G., Kaufman, M. & Thomasson, M. 1993, ApJ, 412, 90
 Heckman, T.M., Armus, L. & Miley, G. K. 1987, AJ, 93, 276
 Heckman, T.M., Armus, L. & Miley, G. K. 1990, ApJS, 74, 833
 Heckman, T.M., Armus, L., Weaver, K. A. & Wang, J. 1999, ApJ, 517, 130
 Hernquist, L., & Katz, N. 1989, ApJS, 70, 419
 Hibbard, J.E., Guhathakurta, P., van Gorkom, J.H., & Schweizer, F. 1994, AJ, 107, 67
 Hibbard, J.E., & Mihos, J.C. 1995, AJ, 110, 140
 Hibbard, J.E., Vacca, W., & Yun, M.S. 2000, AJ, 119, 1130
 Hibbard, J.E., & van Gorkom, J.H. 1996, AJ, 111, 655
 Hibbard, J.E., & Yun, M.S. 1999, AJ, 118, 162
 Mihos, J.C., Bothun, G.D., & Richstone, D.O. 1993, ApJ, 418, 82
 Mihos, J.C., Dubinski, J., & Hernquist, L. 1998, ApJ, 494, 183
 Mihos, J.C., & Hernquist, L. 1996, ApJ, 464, 641 (MH96)
 McGaugh, S.S., & de Blok, W.J.G. 1997, ApJ, 481, 689
 Roberts, M.S., & Haynes, M.P. 1994, ARA&A, 32, 115
 Schiminovich, D., van Gorkom, J. H., van der Hulst, J. M. & Kasow, S. 1994, ApJ, 423, L101
 Smith, B.J., Struck, C., & Pogge, R.W. 1997, ApJ, 483, 754
 Stanford, S.A., & Balcells, M. 1991, ApJ, 370, 118
 Toomre, A., & Toomre, J. 1972, ApJ, 178, 623
 Wright, A.E. 1972, MNRAS, 157, 309
 Yun, M.S. 1999, in IAU Symp. 186, Galaxy Interactions at Low and High Redshift, ed. D. Sanders & J. Barnes (Dordrecht: Kluwer), 81

Wallin, J. F. 1990, *AJ*, 100, 1477

Young, J.S., & Scoville, N.Z. 1991, *ARA&A*, 29, 581

See color Figure 1.

FIG. 1.— The merger evolution of two equal mass disk galaxies with extended gas disks. In this sequence, stars are shown in yellow and gas in blue (where the gas and stars commingle at high density the colors mix to white). Note the development of the gas/star offset in the prograde tail (to the lower right in the bottom panels). Time is noted in each panel; scaled to the Milky Way, the sequence spans approximately 600 Myr.

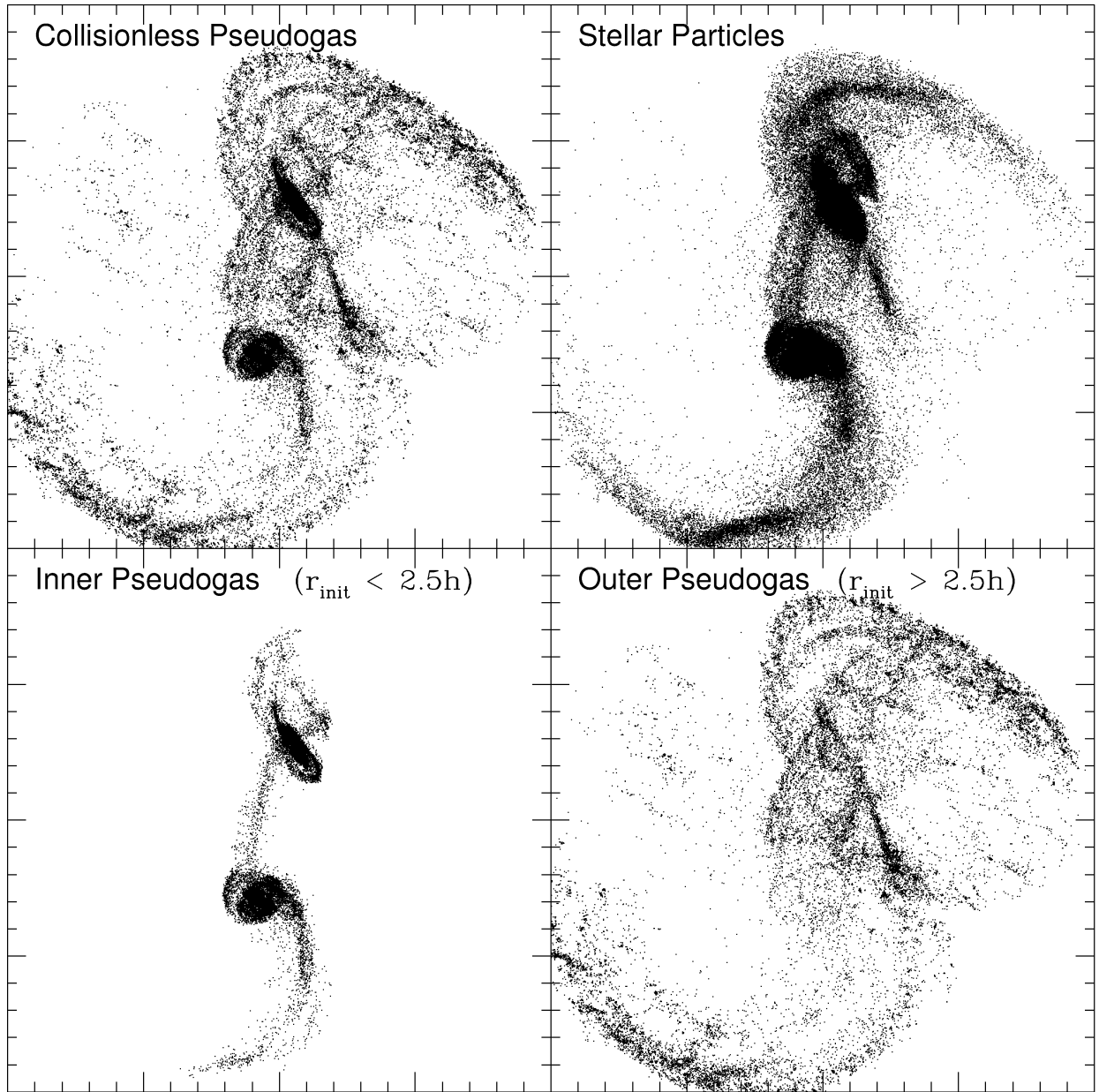


FIG. 2.— A comparison of stellar and pseudogas morphology for a purely collisionless model. “Pseudogas” refers to the gas particles in the full hydrodynamical simulation (Figure 1) which have been converted to collisionless particles to assess the collisionless evolution of extended gas disks (see text). This snapshot corresponds to the final frame in Figure 1. The bottom panels break up the pseudogas into that coming from the inner disk and outer disk respectively, where inner and outer is defined relative to the radius in the progenitor disks where the gas distribution changed from exponential to r^{-1} . In this exercise, no offset is seen between the stars and extended pseudogas.

See color Figure 3.

FIG. 3.— The evolution of a subset of the particles in the prograde tail. a) In a region of the prograde tail showing a strong gas/star offset, stellar (red) and gaseous (blue) particles are identified. b) and c) These particles are then located in the disk at a time approximately one rotation period before the collision. d) The evolution of these particle subsamples, observed in a frame of reference centered on the prograde disk. e) Evolution of the gas subsample and its stellar phase space partners. f) Evolution of the stellar subsample and its gaseous phase space partners. See text for details.

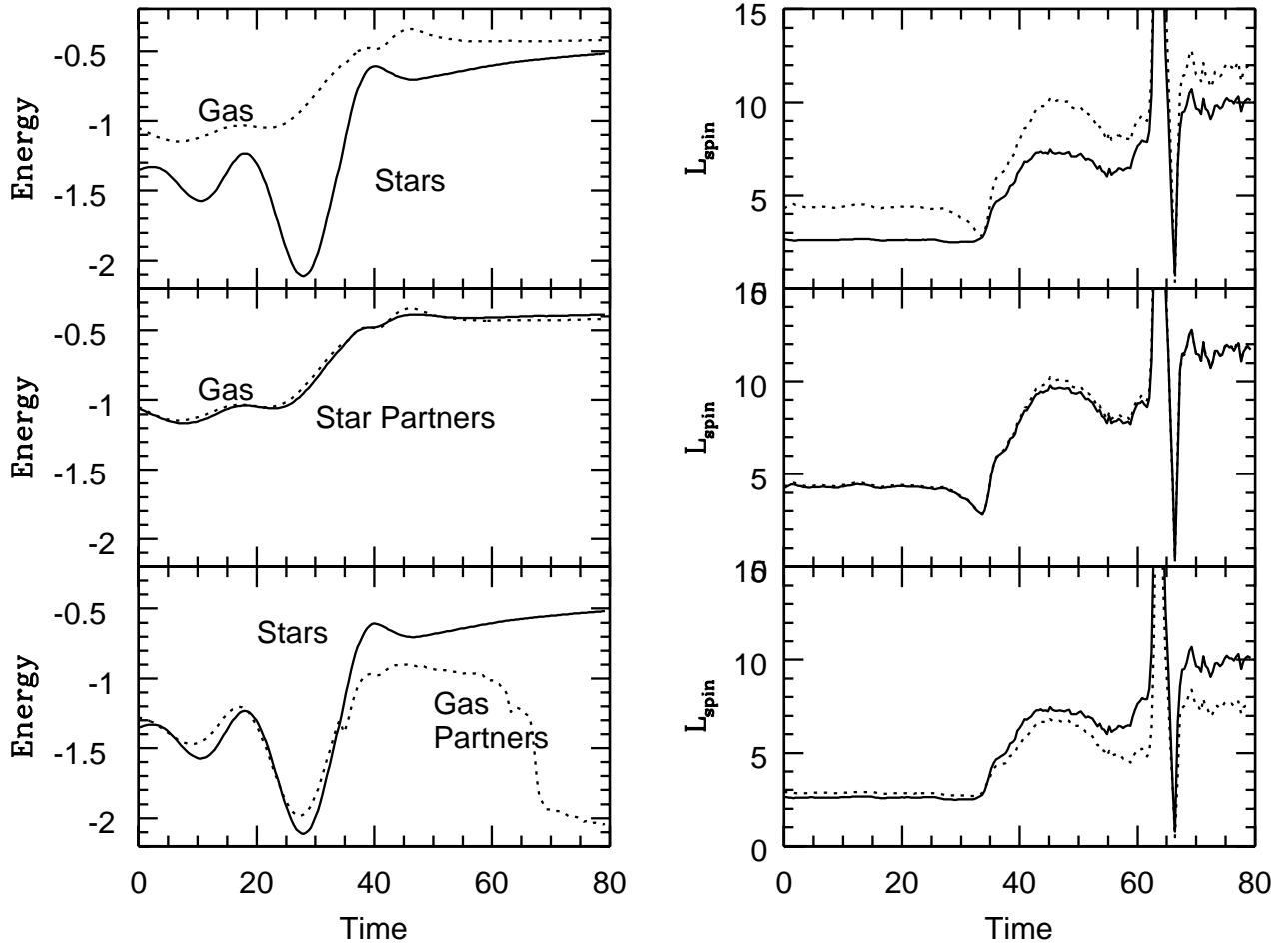


FIG. 4.— Evolution of energy (left panels) and spin angular momenta (right panels) of tail particle subsets. From top to bottom, the panels compare the evolution of the gas and star subsets, the gas and its stellar phase space partners, and the stars and their gaseous phase space partners. In each panel, the gaseous component is shown with a dotted line, while the stellar component is shown with a solid line. Initial impact occurs at $T \sim 30$, while merging happens at $T \sim 65$. In this figure, energy and angular momentum are measured relative to the center of the initial disk.

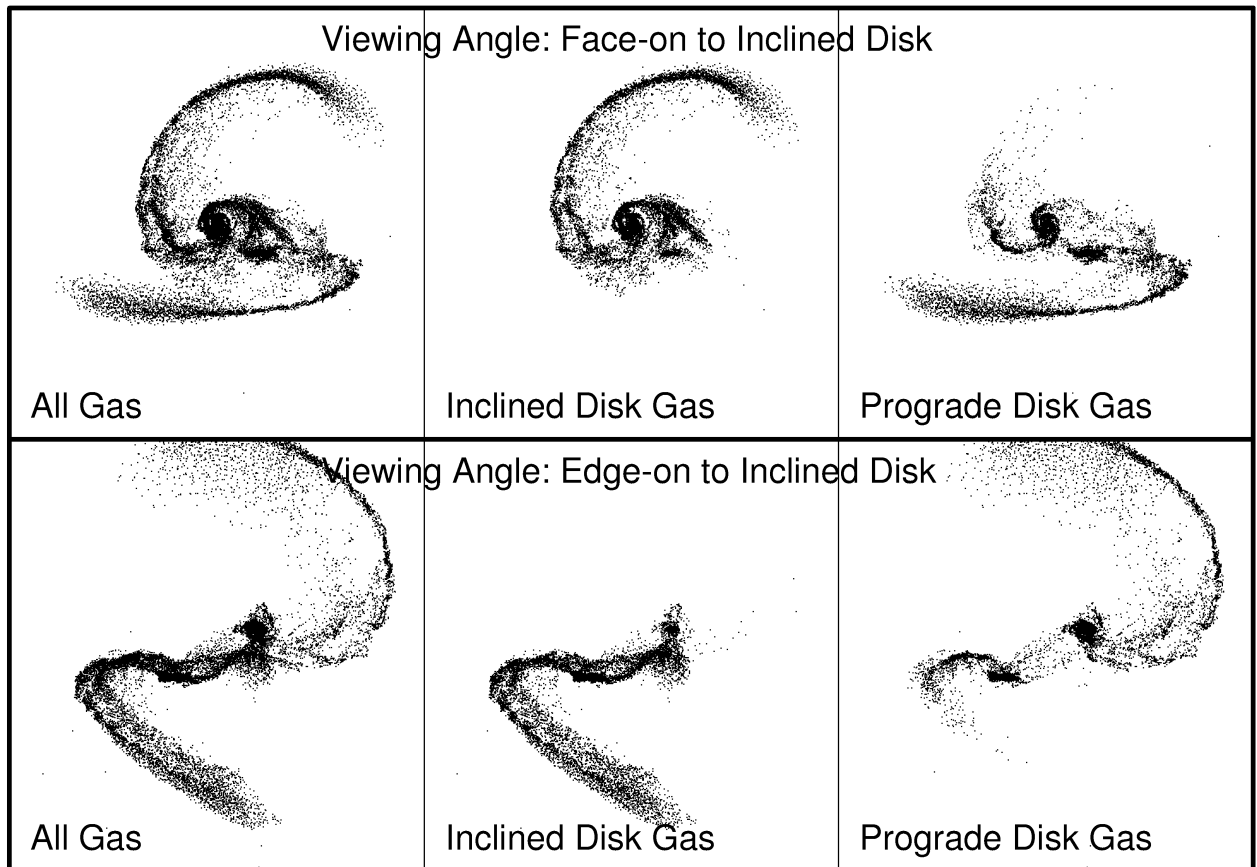


FIG. 5.— Views of the gas in the disk initially inclined to the orbital plane. The top panels show the system rotated so that the inclined disk is viewed face on, while the bottom panels show the system rotated so that the inclined disk is viewed edge on. From left to right, the frames show all the gas, the gas initially in the inclined disk, and the gas initially in the prograde disk. Note the bifurcated tail, the smooth distribution of gas throughout the tail, and the accretion of gas from the prograde disk into the inclined tail.

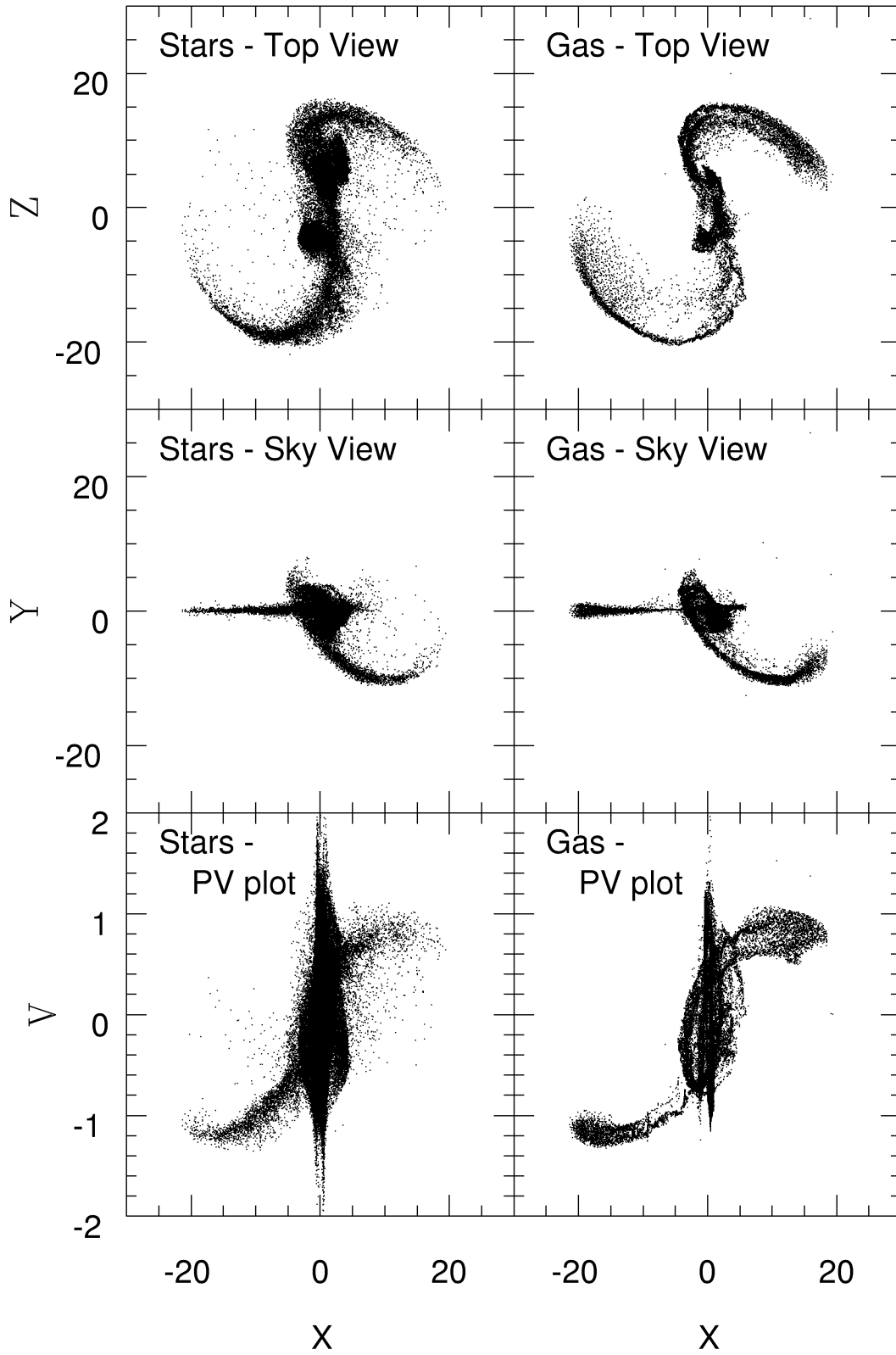


FIG. 6.— A simulated position-velocity plot for the gas and stars in the merger model. The model is observed late in the interaction, at time $T = 53$ when the offset is pronounced, and viewed in the plane of the encounter, along a line of sight where the offset prograde tail is moving towards the observer. The top panels show a top view of the system, while the middle panels show the observed view (i.e. the “sky plane”). The bottom panel shows the observed position-velocity plot. Along the portion of the tail which shows the gas/star spatial offset ($X \sim -5$), kinematic offsets are observed with magnitude $\Delta v \sim 0.3$, or $\sim 60 \text{ km s}^{-1}$ when the system is scaled to the Milky Way.

This figure "fig1.gif" is available in "gif" format from:

<http://arxiv.org/ps/astro-ph/0011131v1>

This figure "fig3.gif" is available in "gif" format from:

<http://arxiv.org/ps/astro-ph/0011131v1>